Deposition and field emission properties of highly crystallized silicon films on aluminum-coated polyethylene napthalate

Junshuai Li[a,b], Jinxiao Wang[a], Min Yin[a], Pingqi Gao[a], Deyan He[a,*], Qiang Chen[b], Hajime Shirai[b]

[a]*Department of Physics, Lanzhou University, 730000 Lanzhou, China*
[b]*Faculty of Engineering, Saitama University, 255 Shimo-Okubo, Sakura, Saitama 338-8570, Japan*

Abstract

Highly crystallized silicon films were deposited on aluminum-coated polyethylene napthalate (PEN) substrates by inductively coupled plasma (ICP-) chemical vapor deposition (CVD) at room temperature. The films with uniform grains about 50 nm have the (1 1 1) preferred orientation. By studying the relation of the silicon film crystallinity to the flow ratio of SiH_4 to H_2, it was found that the interaction between precursors and aluminum layers plays an important role in the crystallization process. The surface roughness of the resultant films was analyzed by atomic force microscopy (AFM). The results reveal that the roughness of the silicon films on aluminum-coated PEN substrates, compared to the films on bare PEN substrates, is dependent on the film phase rather than the substrate morphology. The measurement of field electron emission of the crystalline silicon film indicates that the threshold field is about 8.3 V/μm and the emission is reproducible in the emission region.
© 2007 Elsevier B.V. All rights reserved.

1. Introduction

Low-temperature crystalline silicon thin films have become one of the most promising materials due to their high performance, low fabrication cost and abundant raw materials [1–3]. They have been used in solar cells, thin film transistors, imaging sensors and large-area flat displays. Meanwhile, because of the light weight and flexibility demanded in modern personal information displays, such as e-books, cellular phones, the preparation of high-quality crystalline silicon thin films on plastic has been attracting much attention in these years [4–7]. To date, two approaches are used to manufacture crystalline silicon films on plastic, i.e. laser annealing crystallization (LAC) of amorphous silicon films [6,8] and the deposition of crystalline silicon films assisted with the appropriate substrate temperature, about 100 °C or more, in plasma chemical vapor deposition (CVD) process [4,6,9,10]. However, some drawbacks in the above-mentioned approaches severely block the preparation of high-quality crystalline silicon films on plastic substrates. In LAC process, the fabrication cost is high and the annealing procedure would prolong the period of fabrication. It should be concerned that the sample-transfer process from the deposition chamber to the annealing instrument could bring some contaminations to the silicon films. In reports concerning the deposition of crystalline silicon films on plastic in plasma CVD process, it is necessary to choose the suitable plastic, which cannot deform in the deposition process. At the same time, in order to decrease the bombardment of positive ions and increase the crystallinity

*Corresponding author. Tel.: +86 931 8912172; fax: +86 931 8913554.
E-mail address: hedy@lzu.edu.cn (D. He).

of silicon films, the substrates were usually coated by CeO_2, etc. conductive layers because of the match of crystal lattices between them and crystalline silicon [6].

Considering the wide usage of aluminum as interconnected wires in integrated circuits and the tentative use of low-price plastic, in this paper we tried to perform the direct deposition of crystalline silicon films on aluminum-coated plastic made of polyethylene napthalate (PEN) by ICP-CVD at room temperature. The thickness of the evaporated aluminum film was about 100 nm. It should be worth noting that the Al layer can act as a bar layer to prohibit the contamination to the resultant Si films from the PEN substrates in the initial growth stage. A mixture of SiH_4 and H_2 was used as the source gas. The resultant crystalline silicon films are composed of the uniform grains about 50 nm and the preferred orientation is (1 1 1).

2. Experimental procedure

The plasma was generated by a built-in one-turn inductance coil (in diameter 10 cm) made of a copper tube installed in the reactor. Water was fed in to cool the copper tube in the deposition process. The input power of the 13.56 MHz was 300 W. The total flow of the SiH_4/H_2 mixture was fixed at 20 sccm and the working pressure was about 20 Pa. The dilution of SiH_4 was controlled by regulating the flow ratio of SiH_4 to H_2. In order to create high-density and homogeneous plasma, the inductance coil was coated with a layer of 0.1-cm-thick fiberglass. The base vacuum was 1×10^{-3} Pa. The structure of the samples was characterized by micro-Raman spectroscopy (Jobin-Yvon HR 800), transmission electron microscope (TEM, JEM1200EX) and atomic force microscopy (AFM, CSPM4000).

3. Results and discussions

Fig. 1(a) shows the micro-Raman spectra of sample 1 (S1) and 2 (S2) deposited on bare and aluminum-coated PEN substrates, respectively. The flow ratio of SiH_4 to H_2 was fixed at 4:16 sccm. The thickness of the samples is about 1 μm. Compared to S1, it can be seen that a strong Raman peak centered nearly at 520 cm^{-1} accompanied by a shoulder around 500 cm^{-1} (nano-crystalline phase) for the sample deposited on Al-coated plastic is present, which is attributed to the transverse optical (TO) optical phonon mode in c-Si and suggests that the sample deposited on Al-coated plastic is almost fully crystallized even at room temperature [11,12]. To obtain more information about the microstructure, we performed the TEM measurement on S2. As depicted by the bright field image in Fig. 2(a), it is obvious that the tip of the crystalline grain, like a triangular pyramid, corresponds to Si (1 1 1) crystal orientation. The size of the crystalline grains is uniform and about 50 nm. Fig. 2(b) is the selected-region electron diffraction pattern. It manifests that the film is almost fully crystallized. As calculated, the interplanar distance is about
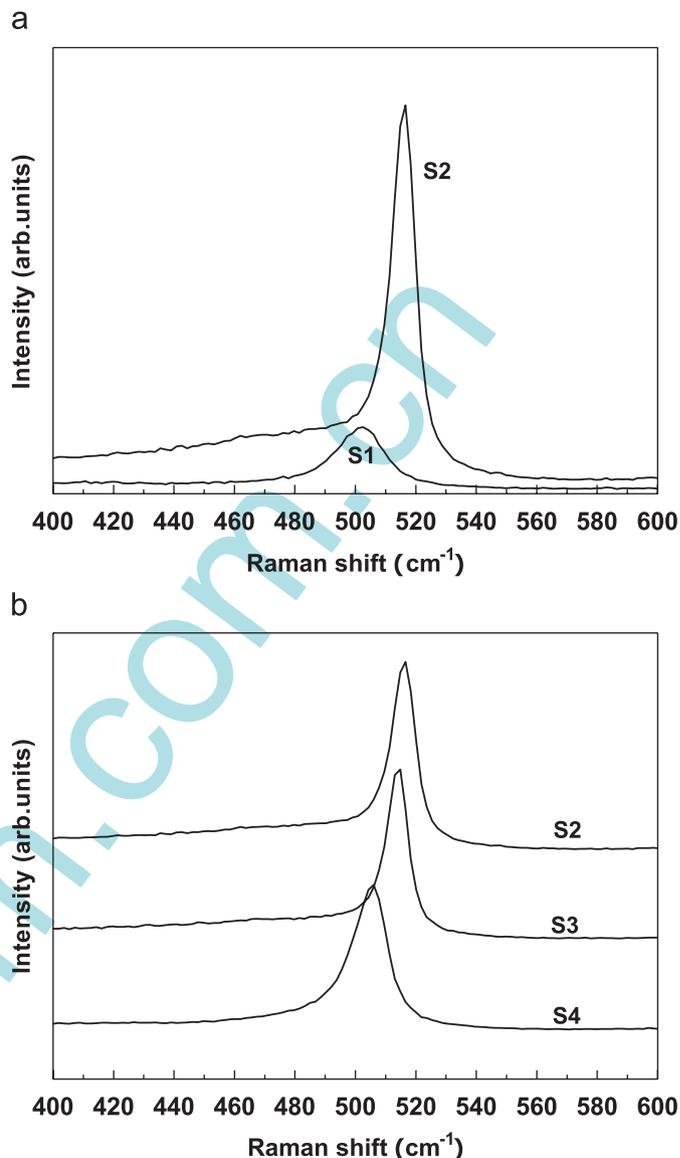

Fig. 1. Raman spectra of S1 and S2 on bare and aluminum-coated PEN, the flow ratio of SiH_4 to H_2 was 4:16 sccm (a) and Raman spectra of S2, S3, S4 on aluminum-coated PEN substrates, the flow ratios of SiH_4 to H_2 were 4:16 sccm, 8:12 sccm and 12:8 sccm, respectively.
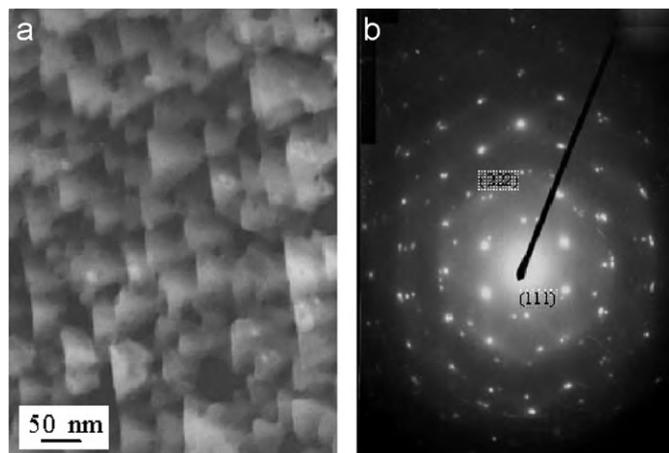

Fig. 2. TEM micrograph of S2: (a) bright field image and (b) selected-region electron diffraction pattern.

0.313 nm and consistent with that of single-crystalline silicon (1 1 1). In general, Fig. 2 demonstrates that the film deposited on the aluminum-coated PEN substrate at room temperature by ICP-CVD is composed of uniform grains and has the (1 1 1) preferred growth orientation.

As reported in the related paper [6], the origin of the growth of the crystalline silicon films on CeO_2, etc. coated plastic substrates is from the enhancement of the nucleation of the crystalline silicon grains due to the lattice match and also from the depression of ion bombardment to the growth surface in the plasma process. However, in the present work, the lattice of the aluminum layer is mismatched with that of crystalline silicon and the substrate temperature is very much lower than that in the previous reports. So there should exit a different crystallization mechanism in the deposition process of crystalline silicon thin films on aluminum-coated plastic at room temperature in ICP-CVD. It is well known that compared to traditional plasma sources, such as capacitively coupled plasma (CCP-) CVD, ICP has the characteristics of high plasma density (about 10^{12} cm^{-3} at 10 mTorr), low electron temperature and the spatial confinement of the discharge, i.e. the plasma is confined around the inductance coil. In the deposition process, increasing the density of SiH_3 and suppressing the densities of SiH_x ($x = 0$–2) are the key to deposit highly crystallized silicon films [13,14]. In virtue of the spatial confinement of the discharge in ICP, the diffusion of SiH_x ($x = 0$–2) to the growth surface can be effectively depressed by adjusting the working pressure and the distance between the inductance coil and the substrate holder. And the strong nonequilibrium chemical processes caused from the high-density electrons in ICP stimulate the interaction between SiH_3 radicals and the aluminum layer, and thus promote the formation of crystalline silicon films. As illustrated in Fig. 1(b) with the increasing flow ratio of SiH_4 to H_2, the shift of Raman scattering peak toward 480 cm^{-1} indicates the decreasing crystallinity. This experimental fact perhaps is due to the remarkable increase of the density of SiH_3 precursors with the increasing flow ratio of SiH_4 to H_2. Therefore, large number precursors impact mutually and cannot effectively interact with the aluminum layer, leading to the decreasing crystallinity of the resultant films. The detailed interaction between SiH_3 and the aluminum layer needs more study.

As one of the important parameters, the surface morphology of the resultant films is closely correlated to the crystallization property of the films and the physical properties of the substrate surface. Figs. 3 and 4 represent the typical three-dimensional (3D) AFM images of the silicon films on bare and aluminum-coated PEN substrates, respectively. As shown in Figs. 3(a) and 4(a), contrasted with the bare PEN substrate, the surface of the aluminum-coated PEN is smoother. However, with changing the film thickness, the surface roughness of the films on the different substrates shows significantly different variation tendency. Fig. 3(b) and (c) shows the surface morphologies of the silicon films on bare PEN substrates with different
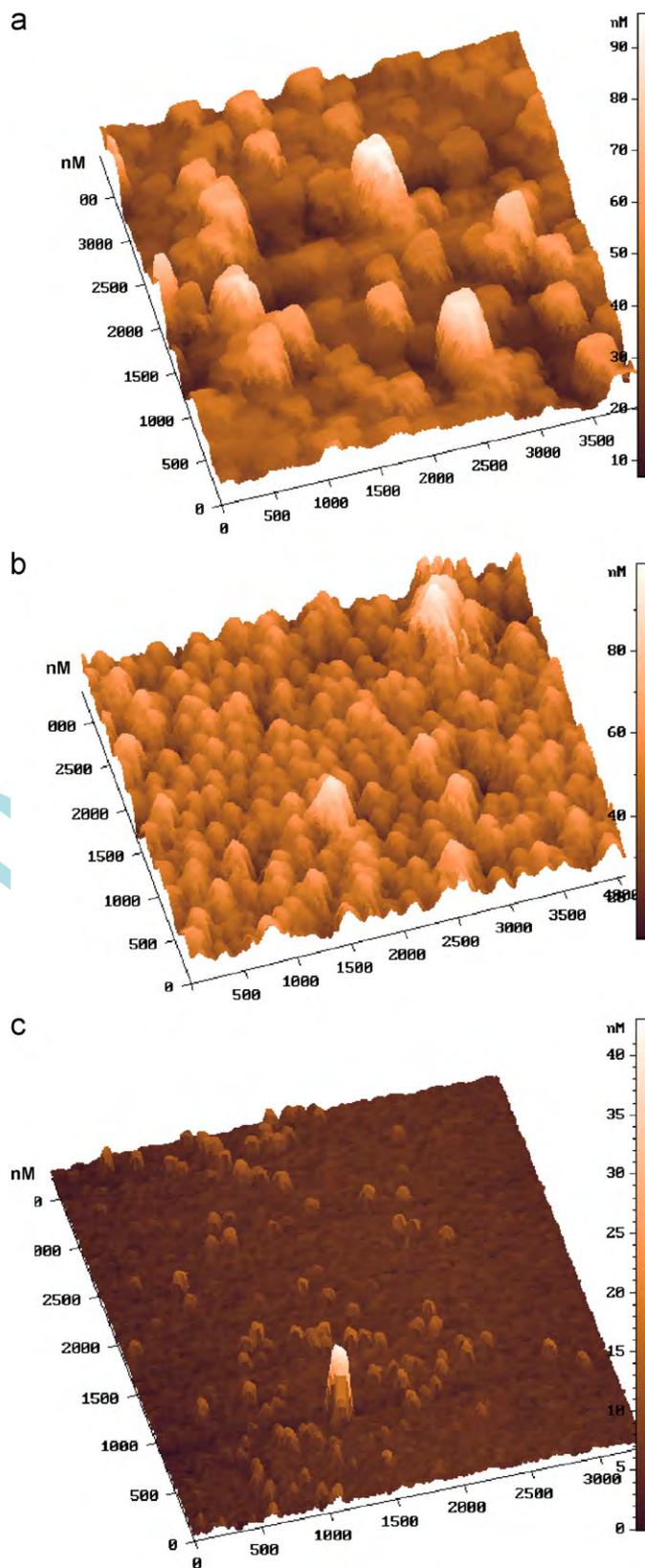

Fig. 3. AFM images of silicon films on PEN: (a) bare PEN, (b) 400 nm silicon film and (c) 1000 nm silicon film.

film thickness, 400 and 1000 nm, respectively. It is obvious that the surface becomes flatter with increasing the film thickness. In the case of aluminum-coated PEN substrates,
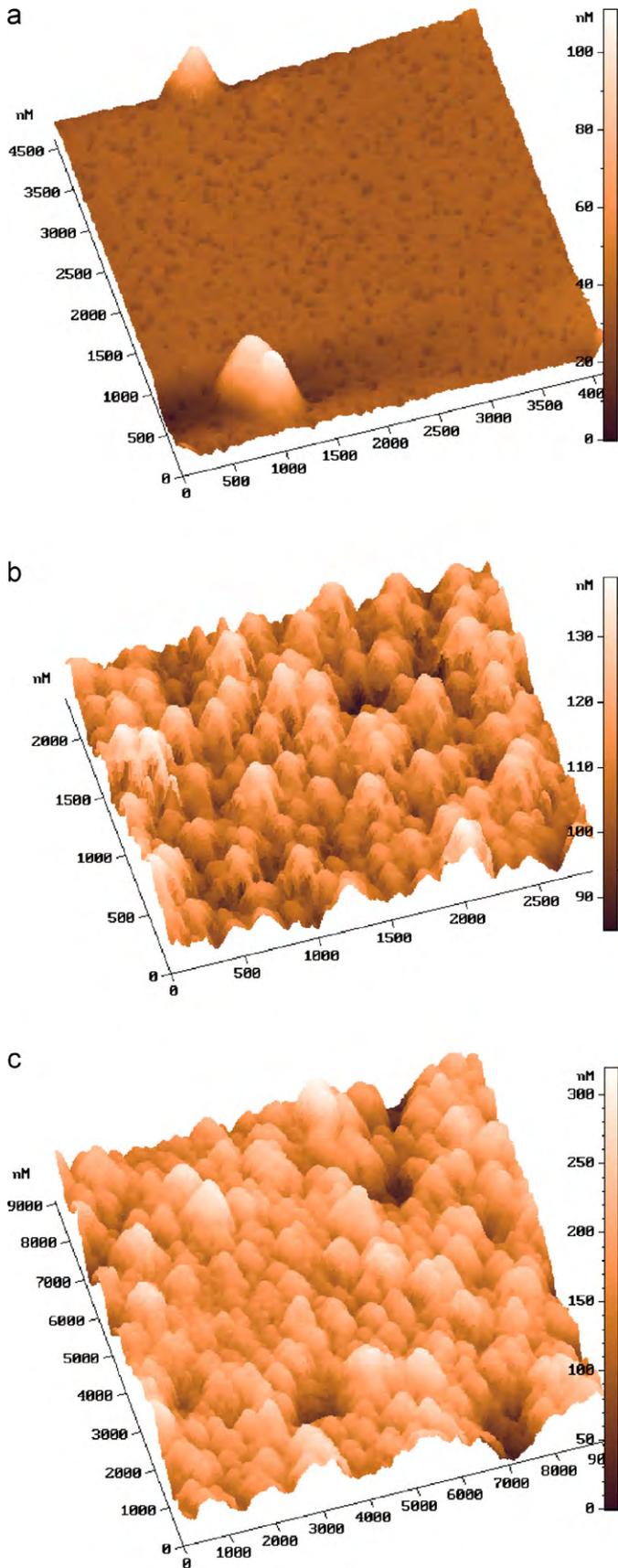
Fig. 4. AFM images of silicon films on aluminum-coated PEN: (a) aluminum-coated PEN, (b) 400 nm silicon film and (c) 1000 nm silicon film.

with increasing the film thickness from 400 nm (Fig. 4(b)) to 1000 nm (Fig. 4(c)), the surface roughness becomes rougher although the substrate is smooth. It is well known that the film surface morphology is closely correlated with the film phase. In the case of silicon films prepared by plasma CVD, the surface morphology of crystalline films is usually rougher than that of amorphous silicon films and with the increase of the crystal grain size, the roughness increases [3,15,16]. In our experiment, compared to the films on the aluminum-coated PEN substrates, the films on bare PEN are mainly composed of nano-phase. When the resultant films are not enough thick, the rough surface morphologies of PEN substrates could be translated to the silicon films and determines the surface roughness of the resultant silicon films. But the surface roughness decreases with increasing the film thickness. On the contrary, to the poly-silicon films on the aluminum-coated PEN substrates, the surface becomes rougher with increasing the film thickness although the substrate surface is smooth.

In the past decade, lots of papers related to the field emission of silicon materials have been published [17–21]. However, there are few reports on the field emission of silicon films on plastic. So we measured the field emission characteristic of S2 in a high-vacuum setup. The crystalline silicon film deposited on the aluminum layer served as a cathode and the distance between the anode and the cathode was fixed at 150 μm using a glass spacer. As shown in Fig. 5, three distinct regions can be seen, corresponding to the zero emission, field emission and current saturation, respectively. The threshold field defined as the electric-field strength at the emission current density of $20\,\mu A/cm^2$ is about $8.3\,V/\mu m$, which is lower than that of conventional micro-fabricated silicon materials whose threshold field is about $20\,V/\mu m$ [19]. It perhaps is because of the natural, uniform cone-shaped micro-structural surface of the film. Especially, it should be pointed out that the field emission
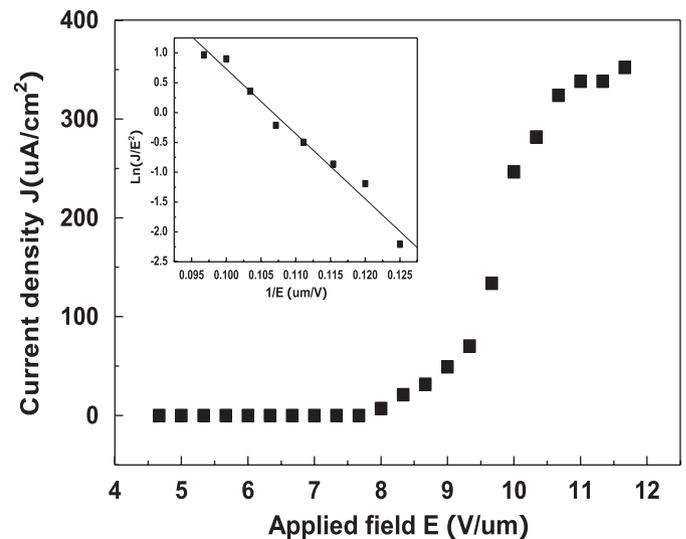

Fig. 5. Current density (*J*)-applied field (*E*) characteristic of S2, the F–N curve of emission region is plotted in the inset.

has good repeatability in the emission region. The inset of Fig. 4 demonstrates the Flower–Nordheim (F–N) plotting of the field emission region. And the plot shows good agreement with the F–N theory. From F–N theory, the slope of the F–N plots, *S*, can be expressed as follows:

$$S = \frac{-B\phi^{3/2}}{\beta}.$$

Here, *B* is a constant with the value $6.831 \times 10^3 \, \text{eV}^{-3/2} \, \text{V} \, \mu\text{m}^{-1}$, ϕ is the effective work function (for silicon, it is about 4.15 eV) [21], β is the field enhancement factor. In our case, the calculated β is about 340. It might be the reason that the crystalline silicon on the aluminum-coated PEN substrate has the lower threshold voltage compared to bulk silicon.

4. Conclusions

In conclusion, highly crystallized silicon thin films were deposited on aluminum-coated plastic at room temperature by ICP-CVD. By analyzing the microstructure of the crystalline silicon films using TEM, it was found that the preferred orientation of the films is (1 1 1) and the films consist of uniform grains with the triangular pyramid shape. The size of the crystal grains is about 50 nm. The thickness-dependent surface morphology evolution measured by AFM reveals that the surface of the crystalline silicon films on the aluminum-coated PEN substrates becomes rougher with increasing film thickness and in the case of bare PEN substrates, the surface becomes smooth, although the substrate roughness can be translated to the resultant silicon film when the film is thin. The successful preparation of highly crystallized silicon films on aluminum-coated plastic at room temperature could provide more choices of substrates and effectively reduce the fabrication cost. The measurement of field electron emission of the crystalline silicon film indicates that the threshold field is about 8.3 V/μm and the emission is reproducible in the emission region.

References

[1] A. Shah, P. Torres, R. Tscharner, N. Wyrsch, H. Keppner, Science 285 (1999) 692.
[2] R.B. Bergmann, Appl. Phys. A 69 (1999) 187.
[3] K. Yamamoto, M. Yoshimi, Y. Tawada, Y. Okamoto, A. Nakajima, S. Igari, Appl. Phys. A 69 (1999) 179.
[4] A.K. Kalkan, S.H. Bae, H.D. Li, D.J. Hayes, S.J. Fonash, J. Appl. Phys. 88 (2000) 555.
[5] S. Wagner, S.J. Fonash, T.N. Jakson, J.C. Sturm, Proc. SPIE 4362 (2001) 226.
[6] D.Y. Kim, M.S. Shim, C.H. Kim, J. Yi, Thin Solid Films 453–454 (2004) 100.
[7] E. Menard, R.G. Nuzzo, J.A. Rogers, Appl. Phys. Lett. 86 (2005), 093507-1.
[8] J.Y. Kwon, D.Y. Kim, H.S. Cho, K.B. Park, J.S. Jung, J.M. Kim, Y.S. Park, T. Noguchi, IEICE Trans. Electron. E88-C (4) (2005) 667.
[9] P. Alpuim, V. Chu, J.P. Conde, J. Non-Cryst. Solids 266–269 (2000) 110.
[10] M. Losurdo, M. Giangregorio, A. Grimaldi, P. Capezzuto, G. Bruno, Eur. Phys. J. Appl. Phys. 26 (2004) 187.
[11] H. Campbell, P.M. Fauchet, Solid State Commun. 58 (1986) 739.
[12] H. Richter, Z.P. Wang, L. Ley, Solid State Commun. 39 (1981) 625.
[13] S. Shimizi, M. Kondo, A. Matsuda, J. Appl. Phys. 97 (2005) 033522.
[14] J. Li, M. Yin, J. Wang, D. He, Chin. Phys. Lett. 22 (2005) 3130.
[15] K. Yamamoto, JSAP Int. 7 (2003) 12.
[16] A. Pleschinger, J. Lutz, F. Kuchar, H. Noll, M. Pippan, Surf. Interf. Anal. 25 (1997) 529.
[17] K. Higa, K. Nishii, T. Asano, Appl. Phys. Lett. 71 (1997) 983.
[18] D.G. Georgiev, R.J. Baird, I. Avrutsky, G. Auner, G. Newaz, Appl. Phys. Lett. 84 (2004) 4881.
[19] S. Johnson, A. Markwitz, M. Rudolphi, H. Baumann, S.P. Oei, K.B.K. Teo, W.I. Mine, Appl. Phys. Lett. 85 (2004) 3277.
[20] M. Kanechika, N. Sugimoto, Y. Mitsushima, J. Appl. Phys. 98 (2005) 054907.
[21] Q. Wang, J.J. Li, Y.J. Ma, X.D. Bai, Z.L. Wang, P. Xu, C.Y. Shi, B.G. Quan, S.L. Yue, C.Z. Gu, Nanotechnology 16 (2005) 2919.